Nuclear Instruments and Methods in Physics Research A 719 (2013) 6–12

Contents lists available at SciVerse ScienceDirect

Nuclear Instruments and Methods in Physics Research A

journal homepage: www.elsevier.com/locate/nima

An accurate and portable solid state neutron rem meter

T.M. Oakes [a], S.L. Bellinger [b], W.H. Miller [a,d], E.R. Myers [c], R.G. Fronk [b], B.W Cooper [b], T.J. Sobering [e], P.R. Scott [c], P. Ugorowski [b], D.S McGregor [b], J.K. Shultis [b], A.N. Caruso [c,*]

[a] Nuclear Science and Engineering Institute, University of Missouri, Columbia, MO, USA
[b] Department of Mechanical and Nuclear Engineering, Kansas State University, Manhattan, KS, USA
[c] Department of Physics, University of Missouri, Kansas City, MO, USA
[d] Missouri University Research Reactor, Columbia, MO, USA
[e] Electronics Design Laboratory, Kansas State University, KS, USA

ARTICLE INFO

Article history:
Received 12 January 2012
Received in revised form
27 February 2013
Accepted 22 March 2013
Available online 13 April 2013

Keywords:
Neutron dosimeter
Solid state neutron detector
Spectrometer

ABSTRACT

Accurately resolving the ambient neutron dose equivalent spanning the thermal to 15 MeV energy range with a single configuration and lightweight instrument is desirable. This paper presents the design of a portable, high intrinsic efficiency, and accurate neutron rem meter whose energy-dependent response is electronically adjusted to a chosen neutron dose equivalent standard. The instrument may be classified as a moderating type neutron spectrometer, based on an adaptation to the classical Bonner sphere and position sensitive long counter, which, simultaneously counts thermalized neutrons by high thermal efficiency solid state neutron detectors. The use of multiple detectors and moderator arranged along an axis of symmetry (e.g., long axis of a cylinder) with known neutron-slowing properties allows for the construction of a linear combination of responses that approximate the ambient neutron dose equivalent. Variations on the detector configuration are investigated via Monte Carlo N-Particle simulations to minimize the total instrument mass while maintaining acceptable response accuracy—a dose error less than 15% for bare ^{252}Cf, bare AmBe, an epi-thermal and mixed monoenergetic sources is found at less than 4.5 kg moderator mass in all studied cases. A comparison of the energy dependent dose equivalent response and resultant energy dependent dose equivalent error of the present dosimeter to commercially-available portable rem meters and the prior art are presented. Finally, the present design is assessed by comparison of the simulated output resulting from applications of several known neutron sources and dose rates.

1. Introduction

The first wide-energy range instrument for measuring neutron dose equivalent was introduced in 1962 by Hankins [1]. The Hankins moderating instrument, building on the ten-inch Bonner sphere response [2], was a paradigm shifting technology in neutron dose equivalent metrology in that the energy dependent dose equivalent [3–5] from thermal to ones-of-MeV could be approximated without directly measuring the neutron energy spectrum.

Since the mid-1960s, five classes of wide-energy range neutron dosimeters have emerged in an effort to improve: (1) the accuracy of measured quantities proportional to neutron energy; (2) the intrinsic detection efficiency; (3) the instrument mass; and/or (4) to extend the neutron energy range. These classes include: single or multiple detectors enclosed by single or multiple neutron interaction materials. In the first class, a combination of boron and/or cadmium, lead or tungsten, and high hydrogen concentration material (usually, high density polyethylene, or HDPE) are used as filters, spallation centers, and moderators to provide ever better response to the dose equivalent curve at up to ones-of-GeV incident neutron energy (e.g., Canberra's SNOOPY or Thermo's SWENDI-II) [6–12]. These instruments are known colloquially as the *Andersson-Braun* (AB) type. The downside of this approach is that the total mass is high (usually >10 kg) and the intrinsic detection efficiency is low (0.25% and 0.05% for the SWENDI-II and SNOOPY, respectively, in response to bare ^{252}Cf). In the second case, multi-band detectors usually tune three or more detectors to the thermal, epithermal, and fast neutron spectrum ranges of the dose equivalent curve using filtering techniques but without extraneous moderator [13–18]. The implication is a lightweight dose equivalent meter (e.g., Ludlum's PRESCILA) but the average dose- and dose-rate error over the thermal to fast range is consequently the highest of the five methods because of severe over or under response in the bands not covered. The third method employs many individual thermal neutron detectors in an HDPE or comparable moderating matrix to provide a depth dependent intensity of thermalized neutrons that yields both the

* Corresponding author. Tel.: +1 816 235 2505.
E-mail address: carusoan@umkc.edu (A.N. Caruso).

0168-9002/$ - see front matter © 2013 Elsevier B.V. All rights reserved.
http://dx.doi.org/10.1016/j.nima.2013.03.060

highest efficiency and lowest average dose- and dose-rate-error of the above methods [19–27]. The shortfall of these instruments is their large moderating volume (usually a 30-cm diameter sphere) needed to accommodate tens-to-hundreds of individual detectors, rendering a non-portable device (>18 kg with electronics). The fourth method utilizes a single position sensitive detector enclosed by moderator and filter materials as an improvement to the classical long counter [28–30]. Although simple, this detection scheme suffers from large moderating volumes and low intrinsic efficiency due to high neutron absorption in the moderator and/or scattering of neutrons outside the detector volume. There are only a few examples of the fifth class which utilize a combination of elements from the first three [31–35]. Like the second class, these dosimeter schemes use a superposition of responses to better approximate the dose equivalent curve, but they incorporate an important improvement in that the overlapping energy response bands are continuous. This provides for a much better dose equivalent match, even up to ones-of-GeV, than that available commercially. The downside is, again, the large total volume and low intrinsic efficiency. Neither the third, fourth, nor fifth device classes have been adopted for commercial production.

Because of need for small detectors, the continued use of gaseous- and scintillator-based thermal neutron detectors in wide-energy, moderating-type neutron dosimeters perpetuates an intrinsic tradeoff between dose error (closest match to the dose equivalent curve), volume of moderator needed, and total detection efficiency (or time/fluence needed to attain reasonable statistics). For the moderating-type classes given above, these tradeoffs can be lessened via a cross-over to solid state methods of neutron detection that allow for a reduced perturbation to the neutron slowing down process (i.e., increased spatial detection resolution) as well as enhancements to intrinsic efficiency [36]. The reduced perturbation stems from the ability to fabricate devices (p–n junctions) nearly wafer thin ($<500\ \mu$m) while retaining high intrinsic efficiency. The high intrinsic efficiency is derived from both the high thermal detection efficiency capabilities (described elsewhere [37]) as well as the detector-moderator geometry (i.e., minimizing neutron absorption in the moderator). The work reported here describes a significantly improved method for measuring the ambient neutron dose equivalent through a combination of superposed detectors and electronic response matching to the dose equivalent standard [38]. The result is a portable instrument that is adjustable to any dose equivalent quantity, but still retains high intrinsic efficiency, and low dose equivalent error for neutrons with energy less than 15 MeV.

2. Design philosophy

The operational quantity devised by the International Commission on Radiation Units and Measurement (ICRU) for operational radiation field measurements is the ambient dose equivalent, $H^*(10)$, which represents the dose equivalent at a point of interest in a radiation field which would be generated at a 10 mm depth in a superimposed tissue-equivalent sphere [39]. For the case of mono-energetic neutrons at energy E, the ambient dose equivalent can be determined by

$$H^*(10) = \Phi h_{cc,E} \tag{1}$$

where Φ is the mono-energetic neutron fluence and $h_{cc,E}$ is a neutron dose-equivalent conversion value specific to the energy of the incident neutrons that accounts for both the quantity of energy absorption and the corresponding relative biological effects (Fig. 1a). Realistic dosimetric applications, however, deal primarily with neutron fields that occupy one or several decades of energy such that is necessary to generalize our expression for the ambient dose equivalent as

$$H^*(10) = \int_0^\infty \Phi(E) h_{cc}(E) dE \tag{2}$$

where $\Phi(E)$ contains the neutron energy characteristics (generally unknown) and $h_{cc}(E)$ is a fluence-to-ambient dose equivalent conversion function. Note that $h_{cc}(E)$ is a highly nonlinear function in energy wherein relatively low dose equivalent per unit neutron fluence (~10 pSv-cm^2) is observed at energies below 10 keV followed by a nearly two order-of-magnitude increase (~600 pSv-cm^2) between 10 keV and 1 MeV as demonstrated in Fig. 1a. This work focuses on $h_{cc}(E)$ data presented by the International Committee on Radiological Protection (ICRP) in publication 74 [4].

Known neutron energy intensity as a function of axial or radial depth into a moderator (Fig. 1b) permits the application of a Fredholm integral equation of the first kind as

$$N(k) = \int_0^\infty R(E,k)\Phi(E) dE \tag{3}$$

where $N(k)$ is the pulse height for energy bin k with a known response matrix R. Such analyses are commonly performed on Bonner sphere systems [2], utilizing multiple diameter spherical moderators to provide different levels of thermalization for incident neutrons—each individual moderator configuration corresponding to an exclusive, energy-dependent thermalization efficiency curve that populates the $R(E,k)$ term (Fig. 1b). Neutrons that thermalize as they reach the instrument's center can be detected and used to populate $N(k)$, thereby transforming Eq. (3) into an ill-posed, under-determined inversion problem [40] requiring a spectral unfolding technique to determine $\Phi(E)$. Solution (s) obtained in this manner are not unique and do not depend continuously on the data such that a more reliable, less computationally expensive method is desirable for real-time dosimetric applications.

The need for a portable, real-time neutron dose-equivalent meter was first addressed by Hankins [1] in the form of a single thermal neutron detector surrounded by moderating material—essentially an adaptation of Bonner's spectrometer utilizing a single, fixed configuration. This "rem meter" exhibits a measurement response

$$M = \int_0^\infty C\Phi(E) d_{cc}(E) dE \tag{4}$$

where C is a calibration constant and $d_{cc}(E)$ is the energy-dependent detector response function. Note the similarity in form between Eqs. (2) and (4). Assuming that the neutron fields are identical, it has been shown that matching the shape of a neutron detector's energy response curve to the fluence-to-ambient dose equivalent conversion function provides an approximate means of determining the neutron dose equivalent without the need to resolve the actual incident energies [6]. A brief comparison of Fig. 1a and b enables the reader to note the similarity in shape between the response of the 10 to 18″ Bonner spheres and the ambient dose equivalent coefficients up to ~8 MeV. The resulting Andersson–Braun design (1963) and its variants (Fig. 2) have been used to formulate several real-time devices including the SNOOPY (1964), LINUS (1975), and WENDI-II (1995) [6–12].

Each of the detector responses shown in Fig. 2 exhibit average errors ranging from 20% to 50% in the thermal and fast regions with considerable error present in the epithermal energy range (i.e., $>950\%$ of $h_{cc}(E)$ for the WENDI-II [4,41–45]). One may conclude that the accuracy of such matching schemes is inherently limited by the use of a single detector and moderator configuration.

In order to accurately match the non-linear shape of the ambient dose equivalent conversion curve (or any future revisions

that may result in its modification – Fig. 1a) it is necessary – in comparison with Bonner's work and as an improvement on the position sensitive long counter [46] – to resolve (within ~1 cm^3) where incident neutrons reach thermal energy in a moderating volume along one or more geometric coordinate axes. For the case of free neutrons travelling in parallel, this task can be accomplished by stacking high thermal efficiency solid state detectors (or comparable thin high thermal efficiency detectors), into an axially symmetric moderator geometry, like that of a right cylinder as shown by Fig. 3a. "Thin" detectors are important as they reduce the neutron scattering perturbation and reduce the total instrument volume. The ~1 cm^3 volume resolution recommendation is chosen as a volume that will yield fine enough scattering length determination to the accurately quantify the neutron dose over many logarithmic energy intervals. The volumetric or three-dimensional resolution comes from stacking (1-D) pixelated (2-D) detectors. By doing so, not only can a real time response be generated, but the conversion curve can also be adjusted electronically. Note, a non-pixilated version, with stacking, that provides only 1-D resolution along the axial coordinate of a cylinder is also possible. Further, it is possible to replace the solid-state detectors, as long as the replacing detector(s) is/are comparably low volume relative to the overall volume and has (or can be summed to provide) at least one-dimensional position sensitivity. In the case of the instrument

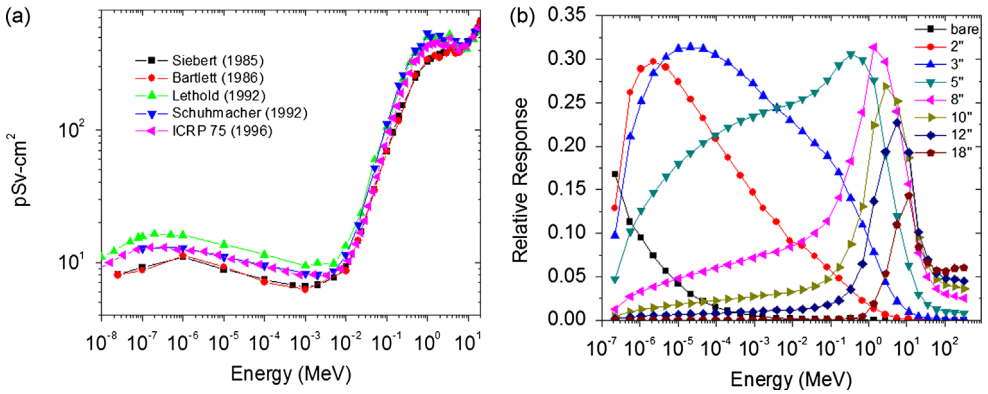

Fig. 1. (a) Various incarnations of the ambient dose equivalent conversion curve (■ Siebert, ● Bartlett, ▲ Lethold, ▼ Schuhmacher, ◀ ICRP 74; adapted from [4,41–45]); (b) response curves from several Bonner sphere configurations.

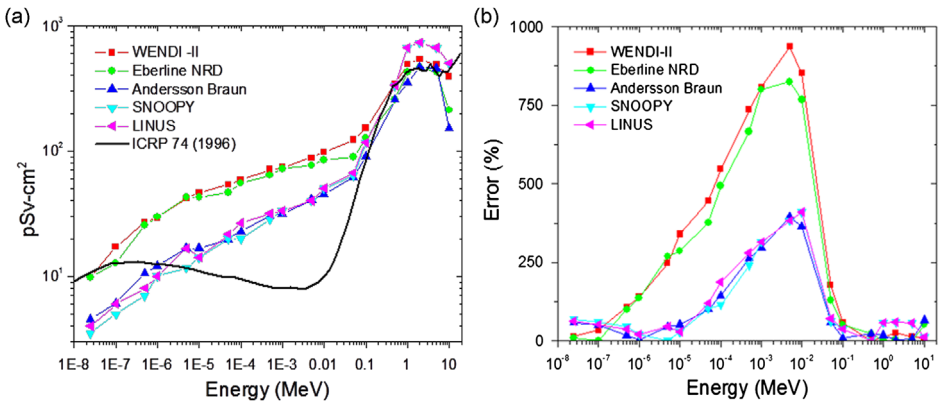

Fig. 2. (a) Calculated neutron-dose-equivalent energy-response for several neutron detection/dosimetry models (■ WENDII-II, ● Eberline NRD, ▲ Andersson Braun, ▼ SNOOPY, ◀ LINUS, — ICRP 74; adapted from [4,6–12]); (b) and their associated error with respect to ICRP 74 fluence-to-ambient dose equivalent conversion values.

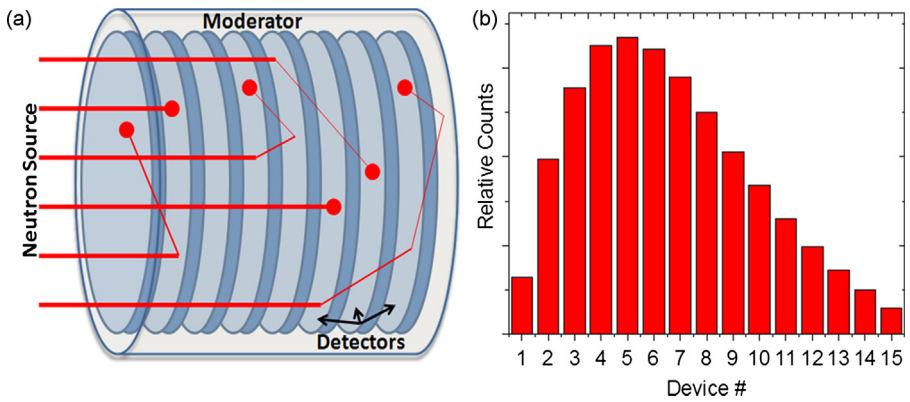

Fig. 3. (a) Adaptation of the Bonner Sphere system into a cylindrical symmetry with solid state thermal neutron detectors allowing for simultaneous detector response as a function of the axial dimension; (b) histogram tallies of measured counts (point of thermalization) from bare ^{252}Cf [48] as a function of axial position into the moderator.

described here, it is assumed that the neutrons are parallel and incident on the front face of the right cylinder as shown in Fig. 3a. In applications with significant scattering, the instrument would be covered by a material that absorbs thermal neutrons, such as cadmium or a boron compound, and the absorbing layer covered with moderator to avoid detecting epithermal and fast neutrons from the sides or back (i.e., a camera geometry). Conversely, if there were very few neutrons and they were incident from all directions, a spherical geometry with radial dependence would be optimal. For the instrument described henceforth, the discussion is focused on the 1-D version (i.e., axial dependence) of the cylindrical geometry wherein n neutron detectors are stacked at 1.0 cm center-to-center spacing and oriented to maintain axial symmetry within a hydrogenous moderator of comparable radius (Fig. 3a and Fig. 4a). Moderator length (axial dimension) is chosen in consideration of the scattering length needed to accurately resolve the dose of 15 MeV neutrons (i.e., ~15.0 cm).

The 1-D axial binning scheme is presented in the form of a histogram in Fig. 3b, unique to the energy and intensity of the incident neutron source (unmoderated ^{252}Cf in this case). The thickness/volume of a solid-state detector is defined by the semiconductor element and any necessary electronics that must be in the neutron path (e.g., preamplifiers, fiberglass boards, etc.). One means of meeting the needed specifications for thermal efficiency, large area and low volume (i.e., thin) are the indirect-conversion, solid state neutron detectors developed at Kansas State University [37]. These microstructured neutron detectors (MSNDs) are comprised of silicon micro-structural trenches, doped and contacted to enable a p–n junction, and backfilled with enriched ^{6}LiF powder. The microstructure dimensions and lower level discriminator settings have been optimized for the ^{6}Li primary reaction products mean free paths to yield devices with 22% thermal neutron detection efficiency. Because standard VLSI methods are used to process the MSNDs, device radii in excess of 10 cm – built either from a single 200 mm wafer or from the superposition of wafer slices from 125 mm wafers – are possible and explored as an upper bound in the calculations described below.

The minimal perturbation of each detector to the moderation process, combined with the high thermal efficiency of each solid-state element, permits the investigation of an individual device's output with respect to the corresponding degree of observed moderator penetration. Energy dependence considerations allow for the delivery of distinct efficiency vs. energy curves as a function of moderator thickness that closely resembles the acquisition from collections of Bonner sphere configurations (Fig. 1a)—but in real time and without the significant non-detectable absorption that occurs in the Bonner Sphere and related instruments.

The availability of n simultaneous measurements from n detectors with unique, Bonner-like response functions permits revision of its rem meter's dose response curve to

$$M = \int_0^\infty \Phi(E) f(d_{cc,1}(E), \ldots, d_{cc,n}(E)) dE \tag{5}$$

where the single detector response curve of a conventional rem meter is replaced by some function, f, of multiple response curves, $d_{cc,1}(E)$–$d_{cc,n}(E)$, to permit more accurate matching to $h_{cc}(E)$. It is proposed that a linear combination of the individual Bonner-like response functions can be used to force the rem meter's overall response function to mimic the shape of the provided fluence-to-ambient dose equivalent conversion function such that

$$f(d_{cc,1}(E), \ldots, d_{cc,n}(E)) = h_{cc}(E) = \sum_{i=1}^{n} g_i d_{cc,i}(E) \tag{6}$$

where g_i is the gain corresponding to the ith detector's response function. It is this gain that allows for the electronic matching to any dose equivalent curve. A collection of measurements from m mono-energetic sources spanning the pertinent energy range are required to populate an m by n matrix, B, where the corresponding $h_{cc}(E)$ values populate a m by 1 column matrix, y. The discrete Fredholm equation is then expressed as

$$y_{(m,1)} = B_{(m,n)} G_{(n,1)} \tag{7}$$

where G is the gain matrix containing n optimal multiplier values (g_1–g_n). Assuming an over-determined system, identification of the optimal gain values is now accomplished by minimization of a "cost" function, selected for this case to be the sum of the square of the residuals

$$J = [y_{(m,1)} - B_{(m,n)} G_{(n,1)}]^T R_{(m,m)}{}^{-1} [y_{(m,1)} - B_{(m,n)} G_{(m,1)}] \tag{8}$$

where R is a diagonal matrix populated by the desired weights, for this case the inverse square values of y [47]. Assuming B is invertible

$$G_{(n,1)} = [B^T_{(n,m)} R^{-1}_{(m,m)} B_{(m,n)}]^{-1} B^T_{(n,m)} R^{-1}_{(m,m)} y_{(m,1)} \tag{9}$$

Once the gain values are determined, the ambient dose equivalent due to a cumulative detector response (i.e., n detectors) can be determined from a series of backward substitutions as

$$H^*(10) = \sum_{i=1}^{n} g_i M_i (\mu\text{Sv}) \tag{10}$$

where M_i denotes the number of counts on the ith detector, or

$$M_i = \int_0^\infty \Phi(E) d_{cc,i}(E) dE \tag{11}$$

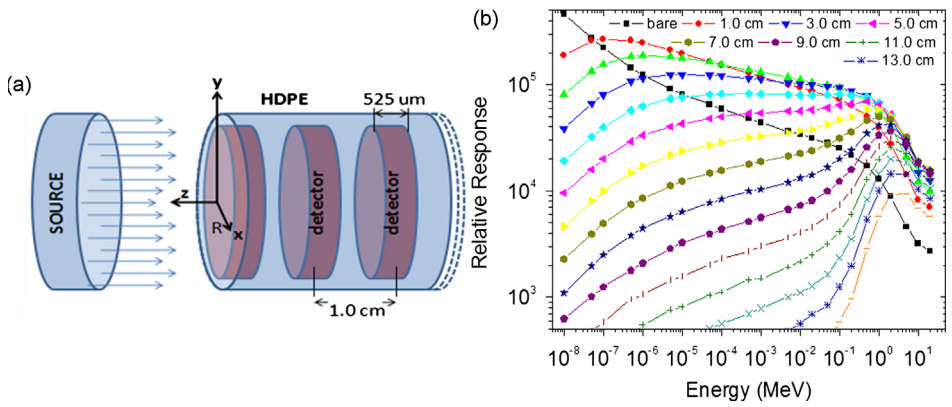

Fig. 4. (a) Generalized MCNPX model schematic for the solid state neutron spectrometer reported here; (b) detector position specific response curves for the $r=10.0$ cm, $L=15.0$ cm configuration.

3. Computational modeling

Instrument studies were performed using the Monte Carlo N-Particle code (MCNP), specifically MCNPX 2.6.0 for charged particle transport. All experiments conducted in the current study utilize a similar, high-density polyethylene moderated model (Fig. 4a) with simulations driven by a planar source of 5000 neutrons per cm^2—in all cases the source radius is set equal to the detector/moderator radius. Neutron detectors are modeled as 525 μm-thick cylinders of natural isotopic abundance silicon containing homogeneously interspersed quantities of neutron-sensitive material sufficient enough to yield 22% thermal detection efficiency, commensurate with the efficiency obtained with the ^{6}LiF solid state detectors developed at Kansas State University [37]. Alpha production in each transduction cell is accounted via series of f4 tallies where a one-to-one ratio exists between realized alpha particles and successfully detected neutrons per the cell material definition. Three sets of primary simulations are conducted on a generalized MCNPX model (Fig. 4a) with $L=15.0$ cm for detector radii of 5.0, 7.0, and 10.0 cm, the latter combination corresponding to a maximum desired moderator mass of 4.5 kg. Each set features a collection of 23 different mono-energetic neutron sources spaced logarithmically between 10^{-8} and 15 MeV with the results compiled into output histograms (one per simulation; see Fig. 3b for an example).

Higher kinetic energy neutrons exhibit larger total path lengths between scattering interactions needed to reach thermal energy, and are therefore capable of further axial penetrations into the detector. This phenomenon yields count distributions (intensity as a function of axial position) that feature markedly different unimodal shapes as a function of energy. Tabulation of the histogram collections permits presentation of the individual device efficiencies as a function of neutron energy (Fig. 4b) that closely resemble the outputs of different Bonner sphere configurations. Note that while the shape remains consistent between the different models, the calculated values appear higher in all cases for larger volume detectors (10.0 cm > 7.0 cm > 5.0 cm) likely due to the subsequent increase in the relative number of probable scattering reactions (i.e., intrinsic efficiency).

Eqs. (6)–(10) are used in conjunction with the data acquired from each simulation set to match the detector response function to the reference $h_{cc}(E)$ curve (Fig. 5) where $n=15$ and $m=23$ (15 devices and 23 appropriately spaced mono-energetic simulations). As shown in Fig. 5a, each of the dosimeter radii exhibit excellent tracking of the reference $h_{cc}(E)$ curve in the range of thermal to 20 MeV. The average errors over the entire energy span measure 10.2%, 10.5%, and 15.7%, respectively, with the absolute maximums observed between 15 and 20 MeV for all cases. These errors are significantly less than those of conventional rem meters displayed in Fig. 2. In addition, the three proposed dosimeters evaluated here have moderator masses of only 1.1, 2.3, or 4.5 kg, depending on the radius utilized. In environments where scattered neutrons may impinge on the side or back of the instrument, the concentric cadmium wrapping and moderator (assuming ~3.0 cm thickness to appropriately thermalize most epithermal neutrons prior to passage through the cadmium layer) will add 1.7, 2.2 or 3.0 kg to the total instrument mass.

4. Model validation and discussion

Validation of the computed ambient dose equivalent is accomplished through superposition of data sets collected from the 23 monoenergetic neutron simulations in Section 3 to emulate four different neutron energy distributions: the first two constructed from the neutron spectra arising from the AmBe and ^{252}Cf sources (Fig. 6a [48]), the third from an unrealistic, entirely epithermal energy range, and the fourth from equal dose contributions of thermal, epithermal, and fast neutrons (Fig. 6b). The individual contributions from each simulation histogram/energy are modified to deliver a net dose of 10 μSv (1.0 mrem).

The histogram data provided by each simulation output is used in conjunction with Eq. (10) to estimate the ambient dose equivalent (Table 1). All of the models/estimates accurately account for the delivered equivalent dose with all observed errors less than 15% for all cases (energy and radii).

Note that most of this error is observed in the AmBe and ^{252}Cf spectra and may be attributed to the fact that the majority of their respective dose contributions are derived from higher energy neutrons where the greatest disparity between $h_{cc}(E)$ and instrument response is observed. Conversely, the doses delivered by epithermal and mixed mono-energetic neutron sources exhibit measurement errors less than 4% and speak directly to the accurate response-matching at energies below 1.0 MeV. Further enhancement to response-matching is likely attainable via design optimization (i.e., different length, radius, detector spacing, etc.) in conjunction with subsequent improvements to Eq. (6) (i.e., perhaps a more complicated function of the different response curves). Further, it is important to note that the current form of Eq. (6) permits both positive and negative multipliers which, with poor counting statistics, could lead to erroneous dose estimates. Although poor counting statistics are mitigated by the high neutron efficiency of this device, this effect will be addressed in future work.

In addition to size, mass, and energy-response characteristics, a rem meter's measurement sensitivity and/or intrinsic efficiency

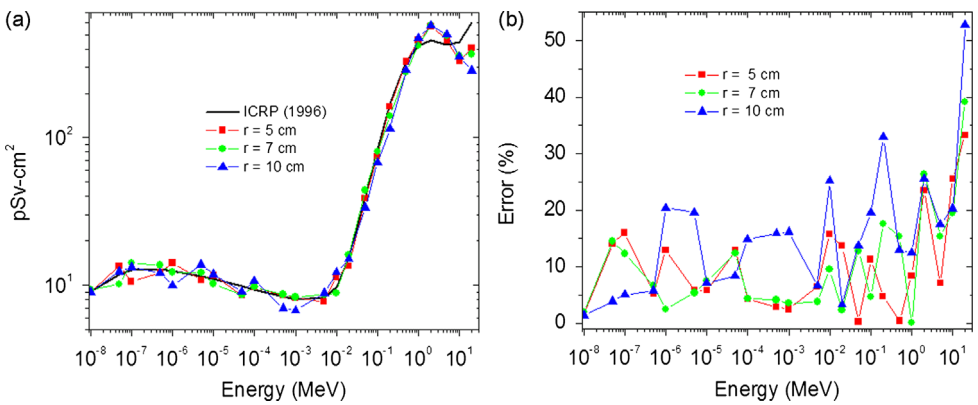

Fig. 5. Response (a) and error (b) of the instrument reported here for $r=5$ (■), 7 (●), 10 (▲) cm and $L=15$ cm. The instrument response in (a) is compared to ICRP 74 fluence-to-ambient dose equivalent conversion values.

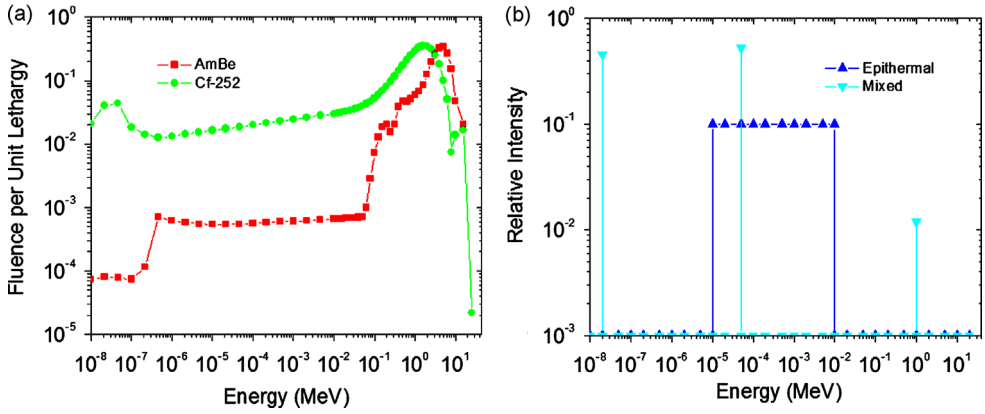

Fig. 6. (a) AmBe (■) and ^{252}Cf (●) source distributions [48]; (b) epithermal (▲) and mixed monoenergetic (▼) source distributions.

Table 1
Error in estimation of reference dose equivalent for neutron source distributions.

Model/source	AmBe (%)	^{252}Cf (%)	Epithermal (%)	Mixed mono (%)
***R*=5.0 cm**	7.5	11.7	2.2	0.1
***R*=7.0 cm**	11.3	8.8	4.0	0.9
***R*=10.0 cm**	13.3	12.0	1.0	0.9

must also be considered when evaluating its overall performance. Canberra's NP2 SNOOPY – an 11.8 kg instrument commonly used for dosimetric surveys of reactor spectra – features a lateral sensitivity of ~10.0 counts/min per μSv/h referenced to ^{252}Cf. Assuming a total side-irradiation (24.38 by 40.64 cm) and 380 pSv-cm^2 average dose-equivalent per unit-neutron-fluence [48], this translates to 0.05% intrinsic efficiency. Despite errors upward of 400% in the epithermal energy region, the SNOOPY reportedly maintains 10% uncertainty with respect to reference dosimetric values (likely due to the generally mid-to-high-range energy spectra to which it is intended to encounter); however, as many real world neutron fields comprise a significant scattering fraction, accurately resolving the epithermal neutron dose equivalent cannot be ignored.

Thermo's WENDI-II incorporates the addition of spallation material (i.e., lead) that extends its energy range upwards of 5.0 GeV for monitoring neutron fields resulting from high-energy accelerators and/or cosmic interactions. The spallation centers consequently increases the total mass to 13.2 kg and increases the epithermal error above 900%. It too maintains a 10% uncertainty to unmoderated spontaneous-fission- or α,n-spectrum-type doses – most likely due to its accurate matching of the dose-equivalent curve at energies greater than 1.0 MeV – and exhibits a lateral sensitivity approximately five times greater than that of the SNOOPY (45.7 counts/min per μSv/h). Given the similar dimensions (22.86 by 33.67 cm) between the two devices, this increase in measurement sensitivity directly corresponds to a five-fold increase in observed intrinsic efficiency to 0.25%.

In contrast to conventional neutron dose-equivalent survey technology, the instrument reported here permits dose-equivalent measurements in the energy range of thermal to 20.0 MeV within 15% accuracy over the total range with less than half of the required mass. All three simulated systems exhibit intrinsic efficiencies to bare ^{252}Cf of 10.25%, 18.89%, and 27.70% (for r=5, 7, and 10 cm, respectively) and measurement sensitivities in terms of raw count data of 353, 6750, and 13,780 counts/min per μSv/h (for r=5, 7, and 10 cm, respectively). This significant increase in instrument sensitivity/intrinsic efficiency related to the SNOOPY or WENDI-II is based on the presence of high thermal efficiency detectors distributed 1 cm along the thermalization path which permit detection of neutrons that are otherwise lost to capture in traditional instruments with a 12 cm moderator radius and single central detector. In concurrence, is important to note that the sensitivities and intrinsic efficiencies of the system described here, solely associated with the deepest detectors, are comparable with those of the SNOOPY and WENDI-II systems (i.e., ~0.25%).

5. Summary and future

A new type of portable neutron rem meter is introduced based on the concept of a solid state neutron spectrometer. The instrument design and algorithm developed are motivated by the high error encountered with commercially available wide-energy range neutron dose equivalent instruments. The device utilizes real-time sampling of thermalized neutrons by multiple weakly perturbing and high thermal efficiency solid-state neutron detectors to provide simultaneous access to a number of Bonner-like response curves. A linear combination of the measurement signals permits excellent matching of the energy-dependent ambient dose equivalent coefficients with average errors less than 15%. Validation of the measured ambient equivalent neutron dose is accomplished using simulation-compiled AmBe, ^{252}Cf, epithermal, and mixed mono-energetic spectra to yield absolute errors less than 15% for all cases. These investigations have yet to consider the propagation of counting statistics on individual detectors to the resulting dose prediction that will be needed to confirm dosimetry accuracy for low flux neutron dose fields and/or short counting times in the 15 s range typically associated with practical neutron dose survey meter applications.

Acknowledgements

The authors acknowledge partial support of this work by the Office of Naval Research under award no. N00014-11-1-0157. ANC wishes to thank Noel Guardala for helpful discussions in originating this work.

References

[1] Dale E. Hankins, Report LA-2717, Los Alamos Scientific Laboratory, Los Alamos (1962).
[2] R.L. Bramblett, R.J. Ewing, T.W. Bonner, Nuclear Instruments and Methods 9 (1960) 1.
[3] ICRP, 2007. The 2007 Recommendations of the International Commission on Radiological Protection. ICRP Publication **103**. Ann. ICRP **37** (2–4).
[4] ICRP, Conversion Coefficients for Use in Radiological Protection Against External Radiation, Publication 74, International Commission on Radiological Protection, Annals of the ICRP, **26**, no. 3/4, Pergamon Press, Oxford, 1996.

[5] J.C. McDonald, B.R.L. Siebert, W.G. Alberts, Nuclear Instruments and Methods in Physics Research Section A: Accelerators, Spectrometers, Detectors and Associated Equipment 476 (2002) 347.
[6] Richard H. Olsher, Hsiao-Hua Hsu, Anthony Beverding, Jeffrey H. Kleck, William H. Casson, Dinnis G. Vasilik, Robert T. Devine, Health Physics 79 (2000) 170.
[7] V. Mares, A.V. Sannikov, H. Schraube, Nuclear Instruments and Methods in Physics Research Section A: Accelerators, Spectrometers, Detectors and Associated Equipment 476 (2002) 341.
[8] C. Birattari, A. Ferrari, C. Nuccetelli, M. Pelliccioni, M. Silari, Nuclear Instruments and Methods in Physics Research Section A: Accelerators, Spectrometers, Detectors and Associated Equipment 297 (1990) 250.
[9] J.M. Brushwood, P.A. Beeley, N.M. Spyrou, Nuclear Instruments and Methods in Physics Research Section A: Accelerators, Spectrometers, Detectors and Associated Equipment 476 (2002) 304.
[10] Chris Benson, Malcolm J. Joyce, Barry O-Connell, Jon Silvie, IEEE Transactions on Nuclear Science 47 (2000) 2417.
[11] M. Cosack, H. Lesiecki, Radiation Protection Dosimetry 10 (1985) 111.
[12] J.W. Leake, Nuclear Instruments and Methods 45 (1966) 151.
[13] J.A. Weaver, M.J. Joyce, A.J. Peyton, J. Roskell, M.J. Armishaw, Review of Scientific Instruments 72 (2001) 2043.
[14] J.A. Weaver, M.J. Joyce, A.J. Peyton, J. Roskell, Nuclear Instruments and Methods in Physics Research Section A: Accelerators, Spectrometers, Detectors and Associated Equipment 476 (2002) 143.
[15] A.M. Williams, N.M. Spyrou, J.M. Brushwood, A. Beeley, Nuclear Instruments and Methods in Physics Research Section A: Accelerators, Spectrometers, Detectors and Associated Equipment 476 (2002) 149.
[16] Gordon K. Riel, Lightweight Neutron Remmeter, United States Patent no. 6930,311 (2005).
[17] R. Olsher, D. Seagraves, S. Eisele, C. Bjork, W. Martinez, L. Romero, M. Mallett, M. Duran., C. Hurlbut, Health Physics 86 (2004) 603.
[18] J. Pope, Radiation Protection Management 11 (1994) 91.
[19] H. Toyokawa, A. Uritani, C. Mori, N. Takeda, K. Kudo, IEEE Transactions on Nuclear Science 42 (1995) 644.
[20] H. Toyokawa, A. Uritani, C. Mori, M. Yoshizawa, N. Takeda, K. Kudo, Nuclear Instruments and Methods in Physics Research Section A: Accelerators, Spectrometers, Detectors and Associated Equipment 381 (1996) 481.
[21] H. Toyokawa, M. Yoshizawa, A. Uritani, C. Mori, N. Takeda, K. Kudo, IEEE Transactions on Nuclear Science 44 (1997) 788.
[22] H. Toyokawa, A. Uritani, C. Mori, N. Takeda, K. Kudo, Radiation Protection Dosimetry 70 (1997) 365.
[23] S. Yamaguchi, A. Uritani, H. Sakai, C. Mori, T. Iguchi, H. Toyokawa, N. Takeda, K. Kudo, Nuclear Instruments and Methods in Physics Research Section A: Accelerators, Spectrometers, Detectors and Associated Equipment 422 (1999) 600.
[24] R.J. Sheu, J.S. Lin, S.H. Jiang, Nuclear Instruments and Methods in Physics Research Section A: Accelerators, Spectrometers, Detectors and Associated Equipment 476 (2002) 74.
[25] J.L. Muniz, M.C. Vincente, E.M. Gonzalez, A.M. Romero, M. Embid, A. Delgado, Radiation Protection Dosimetry 110 (2004) 243.
[26] Taosheng Li, Lianzhen Yang, Jizeng Ma, Dong Fang, Radiation Protection Dosimetry 123 (2007) 15.
[27] Andrew C. Stephan, Vincent D. Jardret, Neutron Detector, United States Patent no. 7514,694 (2009).
[28] Stephen H. Manglos, Neutron Range Spectrometer, United States Patent no. 4837,442 (1989).
[29] Garry B. Spector, Tom McCollum, Alexander R. Spowart, Nuclear Instruments and Methods in Physics Research Section A: Accelerators, Spectrometers, Detectors and Associated Equipment 346 (1994) 273.
[30] Y. Tanimura, J. Saegusa, M. Yoshizawa, M. Yoshida, Nuclear Instruments and Methods in Physics Research Section A: Accelerators, Spectrometers, Detectors and Associated Equipment 547 (2005) 592.
[31] Tom McCollum, Scintillator Fiber Optic Long Counter, United States Patent no. 5298,756 (1994).
[32] D.T. Bartlett, R.J. Tanner, D.G. Jones, Radiation Protection Dosimetry 74 (1997) 267.
[33] M.J. Joyce, B.R. More, D.T. Bartlett, R.J. Tanner, D.G. Jones, Neutron Radiation Detector, United States Patent no. 6362,485 (2002).
[34] S.D. Monk, M.J. Joyce, Radiation Protection Dosimetry 123 (2007) 3.
[35] S.D. Monk, M.J. Joyce, Z. Jarrah, D. King, M. Oppenheim, Review of Scientific Instruments 79 (2008) 023301.
[36] A.N. Caruso, Journal of Physics: Condensed Matter 22 (2010) 443201.
[37] D.S. McGregor, W.J. McNeil, S.L. Bellinger, T.C. Unruh, J.K. Shultis, Nuclear Instruments and Methods in Physics Research Section A: Accelerators, Spectrometers, Detectors and Associated Equipment 608 (2009) 125.
[38] T.M. Oakes, "Modeling and Analysis of a Portable, Solid-State Neutron Detection System for Spectroscopic Applications", Ph.D. Dissertation, 2012.
[39] ICRP, 1990 Recommendations of the International Commission for Radiological Protection, Publication 60, International Commission on Radiological Protection, Annals of the ICRP, **23**, Pergamon Press, Oxford, 1991.
[40] Y. Xu, M. Flaska, S. Pozzi, V. Protopopescu, T. Downar, In: Proceedings of the Joint International Topic Meeting: M&C+SNA (2007) Monterey, California.
[41] A. Ferrari, M. Pelliccioni, Radiation Protection Dosimetry 76 (1998) 215.
[42] H. Schuhmacher, B. Siebert, Radiation Protection Dosimetry 40 (1992) 85.
[43] D. Bartlett, Radiation Protection Dosimetry 15 (1986) 273.
[44] B. Siebert, R. Hollnagel, Radiation Protection Dosimetry 12 (1985) 145.
[45] G. Leuthold, V. Mares, H. Schraube, Radiation Protection Dosimetry 40 (1992) 77.
[46] Y. Tanimura, J. Saegusa, M. Yoshizawa, M. Yoshida, Nuclear Instruments and Methods in Physics Research Section A: Accelerators, Spectrometers, Detectors and Associated Equipment 346 (1994) 273.
[47] Dan Simon, Optimal State Estimation: Kalman, H_∞, and Nonlinear Approaches, John Wiley & Sons, Hoboken, New Jersey, 2006.
[48] IAEA, Compendium of Neutron Spectra and Detector Responses for Radiation Protection Purposes. Technical Reports Series no. 403, Supplement to Technical Reports Series No. **318**. Vienna (2001).